



Computer Vision-Based Sensor of Autonomous Mobile Robot for Detection of Stairs

A.Papsys¹, G.Daunys²

Ph.D. Student, Dept. of Electrical Power Systems, Kaunas University of Technology, Kaunas, Lithuania¹

Professor, Dept. of Electronics and Electrical Engineering, Siauliai University, Siauliai, Lithuania²

ABSTRACT: Autonomous navigation of a robot in an unknown environment is still a challenge for engineers. This paper deals with a simple method for detecting obstacles in a robot's way and stairs in multi-storey buildings. As there may be low light conditions, a structured light-based approach was chosen.

A mathematical model was developed to describe the formation of traces of structured light in images. Various scenarios of a robot's position in relation to stairs were simulated. It was established that light source traces depend on the position and distance of the camera from the light source. Computer simulation revealed characteristic changes of light source patterns in images. It was proved that a cross-form pattern of is attractive for obstacle detection and object recognition.

KEYWORDS: autonomous mobile robot, climbing robot, machine vision, obstacles detection, stair detection

I.INTRODUCTION

One application for robots is to use their ability to move around places that present great danger to humans. An example is the use of a robot in a building in a state of emergency. A robot in such a building is in an unknown environment and needs to autonomously navigate within it. If the building has a number of floors the robot must find the staircase and use it to climb to other floors.

An autonomous mobile robot (AMR) must be supplied with sensors for environment sensing and object recognition. Computer vision is a way to provide flexible, lightweight and accurate sensors, which are very suitable for robots. In this paper was investigated possibility to detect stairs and AMR position respect to stairs using computer vision with active lighting by a laser. An optical system attached to the laser forms cross-hair pattern, which ensures more stable detection of stairs despite of lighting conditions.

The paper is organised as follows. In section II we analyse related work. In section III, we present a mathematical model of the sensor. Results of simulation using the model are presented in section IV. In section V, we compare results of simulation against physical experiments. Section VI concludes the paper.

II.RELATED WORK

We can divide computer vision-based sensors into passive and active. The main feature that separates active from passive sensors is that the former have a light source to brighten the field in front of their cameras.

A typical passive sensor algorithm contains edge detection as pre-processing before feature extraction for object recognition. Edge detection in the case of a staircase image recovers a structure of parallel horizontal lines [1],[2]. The process of implementation could be summarized into three stages [3]. In the first stage, straight lines are detected [4]. The best group of parallel lines or concurrent lines is then extracted [5]. Stage three differs in how the lines are used [2].



International Journal of Advanced Research in Electrical, Electronics and Instrumentation Engineering

(An ISO 3297: 2007 Certified Organization)

Vol. 4, Issue 6, June 2015

Progress in object recognition by computer vision was triggered by the invention of the AdaBoost algorithm with Haar features [6], which was initially applied for face recognition. Afterwards, it was also applied to detect other kinds of objects [7]. Maohai et al [3] proposed the use of AdaBoost for staircase recognition.

Other features for object recognition from a single camera image were proposed. Lowe introduced the SIFT descriptor [8]. Later faster SURF evaluating features were proposed [9]. Dalal and Triggs [10] introduced the Histogram of Oriented Gradient (HOG) descriptor, which with trained SVM could be used for recognition of various objects. Recognition algorithms could benefit from colour information [11].

However, image acquisition by camera is followed by scene depth loss. Three-dimensional data increase the reliability of object recognition. The reliability of computer vision 3D algorithms lies in the success of detecting corresponding points in two or more images. SIFT or SURF features are scale or rotation invariable, hence they are suitable features for 3D vision. Stair detection works can be broadly classified into two types: one combines both image brightness information and range data [12-14], the other uses range information [15]. How to find range data is described in [16],[17]. In most algorithms plane segmentation from range data is used. Extracting planar regions from range data is a well-studied problem [18], for which a “V-disparity” approach was proposed [19].

The company PrimeSense developed a sensor using structured light, which has become the basis for Microsoft Kinect and Asus Xtion sensors. Their primary role is human gesture recognition. Because of their low cost they have become popular in the researcher community as budget devices for object-tracking applications [20]. Research has been done on detecting a stairway using a Kinect sensor [21].

A simplified version is to use a line form laser beam. This method for detecting obstacles was investigated by Csaba et al [22] and Obwald et al [23],[24]. Labecki et al [25] proposed a system with a vertical strip form laser source for stair climbing.

The current research is an extension of structured light-based approaches.

III. MATHEMATICAL MODEL

A laser with an attached optic (later we call it a light emitter) emits rays that have a specific distribution of their propagation directions forming a small dot, a line, a cross or a grid. For further simulation we shall choose a cross (intersection of two perpendicular lines) as a simple form but also a sufficiently informative one. Below we present a mathematical model that describes the formation of a light source trace on 3D objects and an image in a pinhole camera. First we will model traces of light on the 3D objects and afterwards we project the traces onto an image sensor of a pinhole camera.

Let a light emitter centre be at point \mathbf{r}_0 with coordinates x_0 , y_0 , and z_0 . A ray propagation in space could be described by a system of equations using parameter t :

$$\begin{cases} x = x_0 + k_x \cdot t \\ y = y_0 + k_y \cdot t \\ z = z_0 + k_z \cdot t \end{cases} \quad (1)$$

where k_x , k_y and k_z are components of a unit length vector \mathbf{k} , which describes the direction of the ray. The components of the vector satisfy the equation:

$$\sqrt{k_x^2 + k_y^2 + k_z^2} = 1 \quad (2)$$

The ray point on a 3D object is determined as the intersection of the ray direction line with the surface of the object. Let us assume that the surface of the object is bounded by planes parallel to the main coordinate system's planes'. The camera axis orientation is close to the direction of the Y axis. We will describe the bounds of the plane surface by inequalities:

$$x_L \leq x \leq x_R, \quad (3)$$

$$y_C \leq y \leq y_F, \quad (4)$$



International Journal of Advanced Research in Electrical, Electronics and Instrumentation Engineering

(An ISO 3297: 2007 Certified Organization)

Vol. 4, Issue 6, June 2015

$$z_B \leq z \leq z_T, \quad (5)$$

where x_L stands for left X, x_R - right X, y_C - closer Y, y_F - farther Y, z_B - bottom Z, z_T - top Z coordinates.

If the ray from the emitter strikes the vertical plane parallel to the XZ axis, then we can write an equation for parameter t_A :

$$y_t = y_0 + k_y \cdot t_A, \quad (6)$$

where y_t is the Y coordinate of the trace point, and t_A is parameter t for ray A. Equation (6) gives parameter t_A :

$$t_A = \frac{y_t - y_0}{k_y} \quad (7)$$

Substitution of (7) to (1) gives:

$$\begin{cases} x_A = x_0 + k_x \cdot \frac{y_t - y_0}{k_y} \\ y_A = y_t \\ z_A = z_0 + k_z \cdot \frac{y_t - y_0}{k_y} \end{cases} \quad (8)$$

We can describe a structured light source as emitting a stream of N rays, where every indexed ray i ($i=1,2,\dots,N$) has its own propagation orientation $k(i)$. Then (8) can be written as:

$$\begin{cases} x_A(i) = x_0 + k_x(i) \cdot \frac{y_t - y_0}{k_y(i)} \\ y_A(i) = y_t \\ z_A(i) = z_0 + k_z(i) \cdot \frac{y_t - y_0}{k_y(i)} \end{cases} \quad (9)$$

The easiest way to describe a cross form is to describe its points on two perpendicular lines, one of which is vertical and the other horizontal, and both are perpendicular to axis Y of the coordinate system. Such directions of rays could be called primary directions. Other light source orientations are simulated applying a rotation operator for every direction. Initially it is impossible to predict a single plane of the planes bounding an object which would be stroked by trace. Our proposed algorithm calculates the intersection with all possible planes and bounding conditions (3)-(5) are checked. Finally, for every ray only one point is left, whose distance to the camera is smallest.

The obtained cloud of points in the 3D scene are projected to the pinhole camera using perspective projection.

IV.RESULTS OF SIMULATION

The described model was implemented using *MathWorks Inc* MATLAB[®]. The model helped us to obtain images of a cross-hair laser beam trace (we will call it an optical marker or OM for short) on the scene where a robot with a structured light sensor moves. One of the goals of the simulation was to find the best disposition of a camera and a light emitter on the robot.

A trivial disposition is obtained when a light emitter sits in the central line of a camera view. In this case the camera always acquires an image of a cross with two perpendicular lines despite the obstacles. Therefore the centre of the light emitter must be shifted from the centre of the camera.

First we describe the results when the centres of the camera and light emitter are at the same height but are shifted in a horizontal direction perpendicular to the direction of sight. Also, optical axes of the camera and light emitter are parallel (their angular coordinates are equal).

International Journal of Advanced Research in Electrical, Electronics and Instrumentation Engineering

(An ISO 3297: 2007 Certified Organization)

Vol. 4, Issue 6, June 2015

One example of a simulated trace of OM on a flat surface is shown in Figure 1. It reveals that lines in an image are not perpendicular when there is a shift between the camera and laser centres. An angle between lines depends on the distance of the laser from the camera. This dependence is shown in Figure 2. When the displacement of camera and light emitter centres is small the angle between cross lines is close to 90 degrees. It decreases approximately linearly with an increase in the distance between the camera and the emitter. When the displacement exceeds 20 cm, the angle decrease becomes slower.

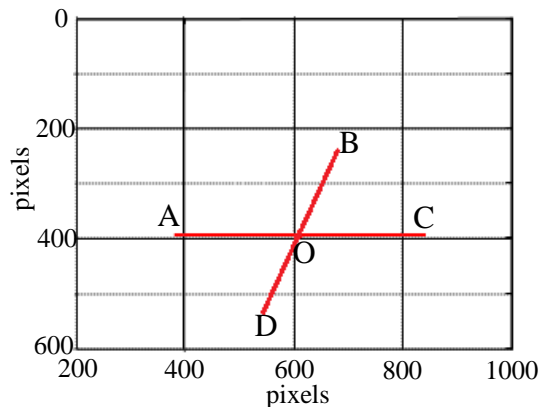


Fig. 1 Simulated trace of structured light (cross) on flat surface when distance between camera and laser is 20 cm, and camera and emitter are oriented by 10 degrees down

We can split the optical marker form from Figure 1, which was obtained on a flat surface, into four sections, OA, OB, OC and OD, with a common point O.

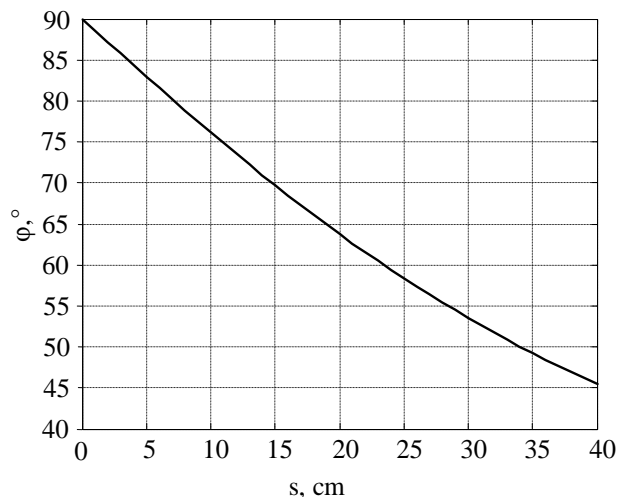


Fig. 2 Angle between lines of the cross versus distance between camera and laser, when camera and emitter are oriented by 10 degrees down

The next simulated situation is when a robot with an attached system is approaching a wall (plane in front of robot is bent up by 90 degrees). The image of the simulation is shown in Fig. 3. The simulation was done when a camera and an emitter were oriented by 10 degrees down. When the distance from the system to the wall reduces, the OM from the floor climbs up the wall. The vertical line of the OM (its OB section) in the image becomes broken. The part of the OB section that projects on the wall becomes vertical in the image. The coordinates of the point, in which the direction of the OB section changes, are cues for triangulation to calculate a distance from the AMR to the wall.

International Journal of Advanced Research in Electrical, Electronics and Instrumentation Engineering

(An ISO 3297: 2007 Certified Organization)

Vol. 4, Issue 6, June 2015

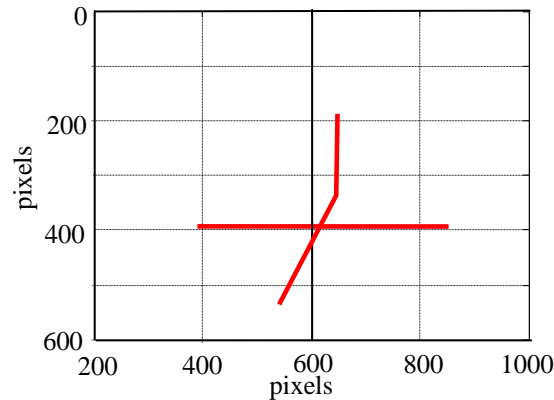


Fig. 3 Results of simulation when a wall is in front of a system

More detailed views of simulation results of cross image versus robot distance from wall are shown in Figure 4. There images shown are acquired by a camera, when the distances from the wall are 3.0, 2.5, 2.0 and 1.5 metres. When the robot moves toward a wall and the horizontal OM line (line AC) projects on the wall, AC in the image starts to move down (Y coordinate in image increases).

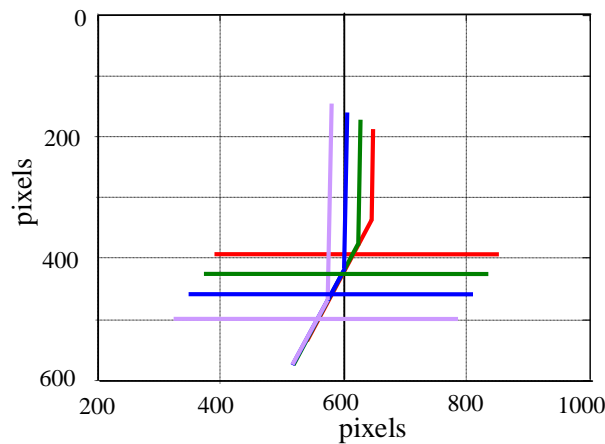


Fig. 4 Results of simulation when a wall is in front of a system. Traces shown when system is at distances of 3.0, 2.5, 2.0 and 1.5 meters from the wall

A model of stairs used in a computer simulation is shown in Fig. 5. Simulated OM images on ascending stairs are shown in Figs. 6–8. In the case of Fig. 6, the AMR is in front of the stairs ($\beta = 180^\circ$). This is the desired orientation before the AMR starts to climb. In Fig. 7, the AMR orientation relative to the stairs is 160° . The comparison of OM forms in the figures reveals that this orientation could be tracked by angle ϕ , whose dependence versus orientation is plotted in Fig. 9. In Fig. 8, AMR orientation is close to parallel to the stairs ($\beta = 100^\circ$). In this case the OM form changes more drastically.

International Journal of Advanced Research in Electrical, Electronics and Instrumentation Engineering

(An ISO 3297: 2007 Certified Organization)

Vol. 4, Issue 6, June 2015

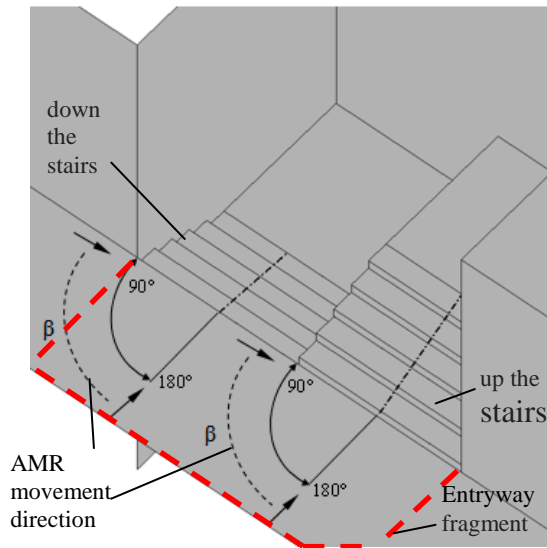


Fig. 5 Model of stairs used for computer simulation. Solid arcs show angle of AMR position relative to stairs (β)

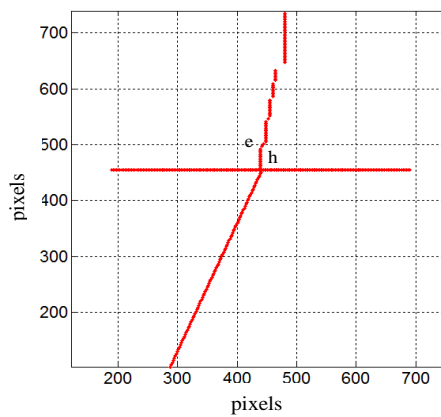


Fig. 6 Computer modelling of OM form on stairs when $\beta = 180^\circ$ (ascending stairs)

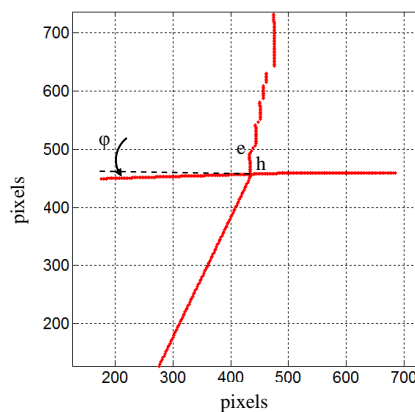


Fig. 7 Computer modelling of OM shape on ascending stairs when $\beta = 160^\circ$

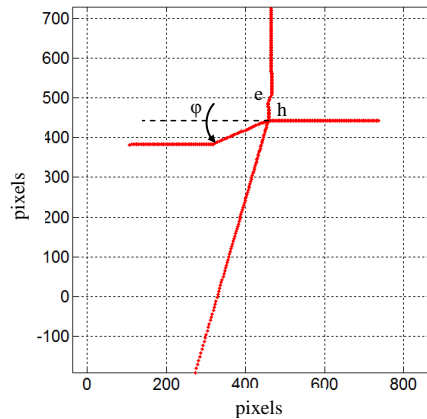


Fig. 8 Computer modelling of OM shape on ascending stairs when $\beta = 100^\circ$

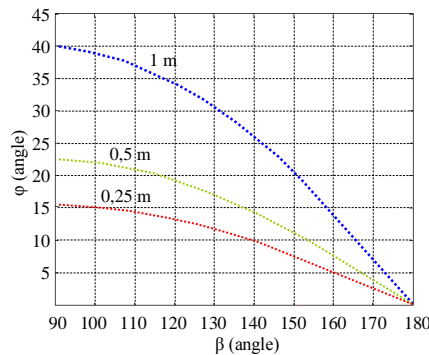


Fig. 9 Dependence of angle between the OM sections OA and OB versus AMR orientation to ascending stairs

Computer simulation results for descending stairs are shown in Figs. 10–13. Summarizing the computer simulation for both types of stairs (ascending and descending), when the AMR is on the left, we can conclude that OM sections OC and OD remain unchanged because due to the selected AMR and stairs layout, OM does not strike the stairs. In the case of AMR localization on the right, the unchanged sections would be OA and OD (because of symmetry). In all cases the OB section transforms to a polygonal line. When there is a straight angle between the AMR and the stairs construction, transformation occurs only in section OB, which becomes split into parts with different numbers of pixels. Interruptions between intervals indicate that OM strikes planes at different heights.

Evaluation of stair parameters can increase evidence of the presence of stairs in front of the AMR. Most expected stair run length e intervals are from 20 cm to 36 cm and riser height h intervals from 12 cm to 20 cm.

International Journal of Advanced Research in Electrical, Electronics and Instrumentation Engineering

(An ISO 3297: 2007 Certified Organization)

Vol. 4, Issue 6, June 2015

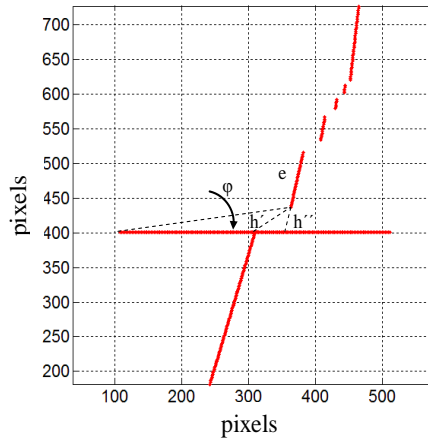


Fig. 10 Simulated OM form on the stairs when $\beta = 180^\circ$ (descending stairs)

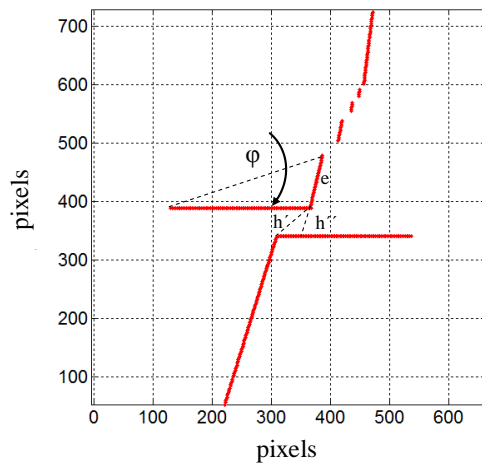


Fig. 11 Simulated OM form on the stairs when $\beta = 160^\circ$ (descending stairs)

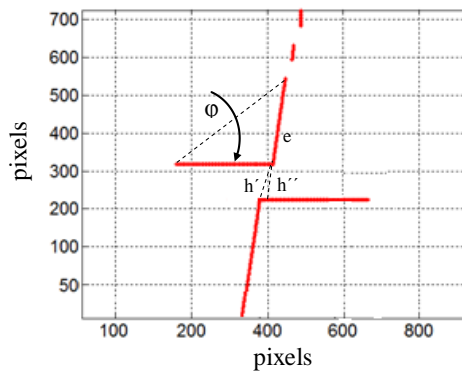


Fig. 12 Simulated OM form on the stairs when $\beta = 100^\circ$ (descending stairs)

International Journal of Advanced Research in Electrical, Electronics and Instrumentation Engineering

(An ISO 3297: 2007 Certified Organization)

Vol. 4, Issue 6, June 2015

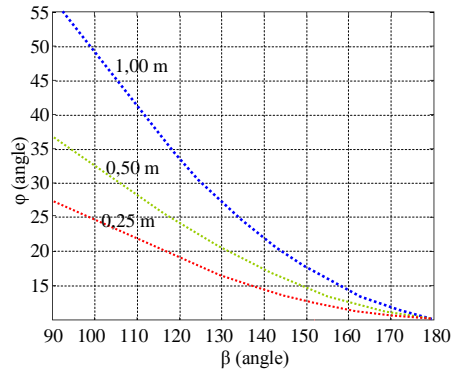


Fig. 13 Dependence of angle between the OM sections OA and OB versus AMR orientation to descending stairs

Orientation of the AMR relative to stairs can be obtained from the dependence of angle ϕ versus AMR orientation to stairs (see Fig. 9).

V. RESULTS OF PHYSICAL EXPERIMENT

A physical experiment on the AMR supplied with OM was carried out on the constructed staircase with dimensions in accordance with the typical stair data. The experimental images are shown in Fig. 14 (ascending stairs). A comparison of the computer simulation and physical experiment is presented in Table 1. The measured dimension dependence on AMR orientation is shown in Fig. 15.

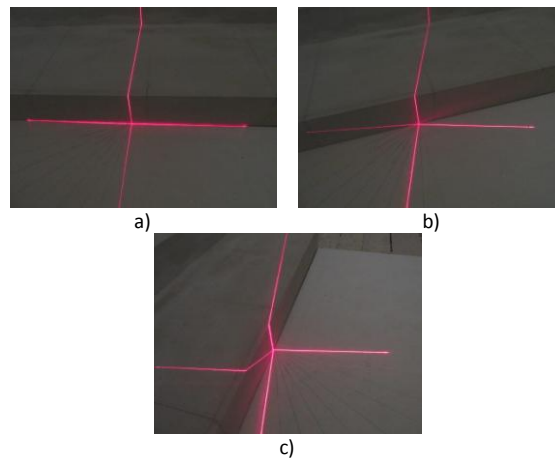


Fig. 14 OM form on the ascending stairs when the distance between the laser and OM centre is 100 cm and angle β : a) 180°, b) 160°, c) 100°.

Image analysis revealed that a riser height h can be evaluated with reasonable accuracy when the AMR orientation angle with respect to the axis directed to stairs is greater than 95°. For the evaluation we need to know the distance from the AMR to the OM centre O and the length of the first part of the broken section OB in the image expressed in pixels. When the angle of AMR orientation is less than 95°, section OB of OM does not fall on stairs and it remains straight. In this case section OA is broken, and riser height h can be found using Pythagoras' theorem. Stair depth e can be evaluated using the distance from the AMR to the OM centre O and the length of the second part (counting from the centre O) of the polygonal line OB evaluated in pixels. When the AMR is rotating the mentioned part of the polygonal line becomes longer. Its length is evaluated according to the AO section rotation by angle ϕ . A more complex algorithm is needed when the angle is less than 140°. It is impossible to find the end of the second part of OB, therefore the length is undefined. On the other hand, now section OA is transformed to a polygonal line. We recognize that a stair is in

International Journal of Advanced Research in Electrical, Electronics and Instrumentation Engineering

(An ISO 3297: 2007 Certified Organization)

Vol. 4, Issue 6, June 2015

image by a disposition of two planes by distance h .

TABLE I. COMPARISON OF SIMULATED AND MEASURED VALUES FOR ASCENDING STAIRS

No.	Angle				Length	
	AMR position (β°)	Measure d (ϕ°)	Calculate d (ϕ_s) $^\circ$	Angle error ($\phi_M - \phi_s$)	Stair run (e) cm	Rise height (h) cm
1.	180	0	0	0	30.8	17.3
2.	170	7	6.8	0.2	30.8	17.4
3.	160	14	13.2	0.8	30.8	17.6
4.	150	21	20.1	0.9	30.9	17.7
5.	140	27	26.2	0.8	30.9	17.7
6.	130	30	30.9	0.9	32.3	17.7
7.	120	34	33.2	0.8	33.5	17.8
8.	110	37	36.6	0.4	34.6	17.8
9.	100	40	39.1	0.9	38.7	17.8

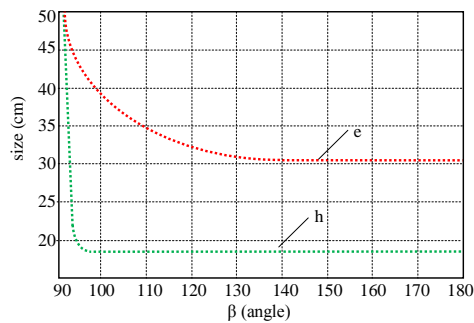


Fig. 15 Ascending stair measured dimension dependence versus the orientation of the AMR when the distance between the laser and the OM centre is 100 cm

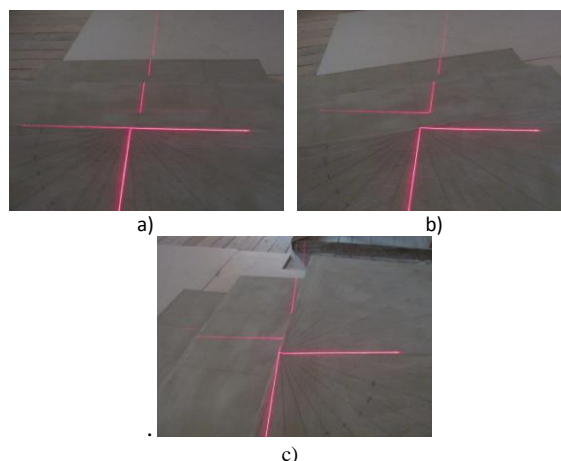


Fig. 16. OM form on the descending stairs when the distance between the laser and OM centre is 100 cm and angle β : a) 180°, b) 160°, c) 100°

Image analysis of the physical experiment data revealed that riser height h could be accurately evaluated when the AMR orientation was in the range $[100^\circ - 180^\circ]$ in respect of stairs. Stair depth e could be evaluated in the range $[115^\circ - 180^\circ]$. The presence of stairs in the visual field of the AMR camera is confirmed by interruptions of sections OA or

International Journal of Advanced Research in Electrical, Electronics and Instrumentation Engineering

(An ISO 3297: 2007 Certified Organization)

Vol. 4, Issue 6, June 2015

OB. They show that horizontal planes are at different heights. OM analysis is done only in the first sections from the centre O because only their lengths could be measured accurately. The results of stair dimension measurement for descending stairs are presented in Table 2. The dimension dependence on AMR orientation is shown in Fig. 17.

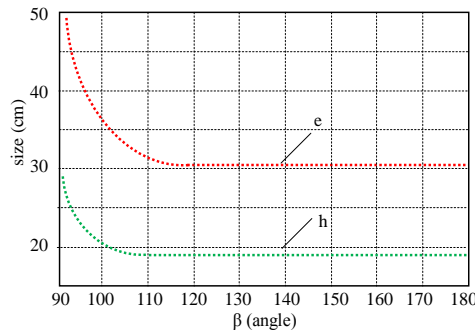


Fig. 17 Descending stair dimension dependence versus the orientation of the AMR when the distance between the laser and OM centre is 100 cm

TABLE II. COMPARISON OF SIMULATED AND MEASURED VALUES FOR DESCENDING STAIRS

No.	Angle				Length	
	AMR position (β°)	Measure d (φ°)	Calculate d (φ_s°)	Angle error ($(\varphi_M - \varphi_s)$)	Stair run (e) cm	Rise height (h) cm
1.	180	12	10.6	1.4	31.7	18.3
2.	170	14	12.8	1.2	31.6	18.3
3.	160	16	14.8	1.2	31.4	18.4
4.	150	19	17.6	1.4	31.4	18.4
5.	140	23	21.4	1.6	31.5	18.5
6.	130	27	25.9	1.1	31.4	18.4
7.	120	33	31.2	1.8	31.6	18.5
8.	110	39	37.6	1.4	32.5	18.6
9.	100	51	49.5	1.5	36.8	21.7

VI. CONCLUSION

The results of simulation revealed that a structured light pattern in a cross-hair form can help to detect obstacles in a robot's way and also the stairs for climbing. Shifting a light emitter in both horizontal and vertical directions in relation to camera position creates richer features images for recognition of obstacles or stairs. The developed method enables evaluation of distance to stairs, depth of stair and height of riser. Relative errors for ascending stairs are smaller (2.8% for e , 1.9% for h) than for descending stairs (5.0% for e , 2.3% for h).

REFERENCES

- [1] Cong, Y., Li, X. M., Liu J., and Tang Y. D., "A stairway detection algorithm based on vision for UGV stair climbing," in Proc. of IEEE Int. Conf. on Networking, Sensing and Control (ICNSC 2008), Sanya, China, pp.1806–1811, 2008.
- [2] Molton, N., Se, S., Brady, M., Lee, D., and Probert P., "Robotic sensing for the partially sighted," Robotics and Autonomous Systems, Vol.26, pp.185–201, 1999.
- [3] Maohai, L., Han, W., Lining, S., and Zesu, C., "A robust vision-based method for staircase detection and localization," Cognitive Processing, Vol.15, issue 2, pp.173-194, 2014.
- [4] Lu, G. Q., Xu, H. G., and Li, Y. B., "Line detection based on chain code detection," in Proc. of IEEE Int. Conf. on Vehicular Electronics and Safety, China, Xian, pp.98–103, Oct. 2005.
- [5] Tuytelaars, T., Van Gool, L., Proesmans, M., and Moons, T., "The cascaded Hough transform as an aid in aerial image interpretation," in Proc. of 6th Int. Conf. on Computer Vision, India, Bombay, pp. 67–72, Jan. 1998.
- [6] Viola, P., Jones, M., "Rapid object detection using a boosted cascade of simple features," in Proc. of 2001 IEEE Conf. on Computer Vision and Pattern Recognition (CVPR), Kauai, USA, Vol.1, pp.511–518, 2001.
- [7] Lienhart, R., Jochen, M., "An extended set of Haar-like features for rapid object detection," in Proc. of Int. Conf. on Image Processing, vol.1, pp. I-900, IEEE, 2002.
- [8] Lowe, D. G., "Object recognition from local scale-invariant features," in Proc. of the 7th IEEE Int. Conference on Computer Vision, Vol.2, pp.1150–1157, 1999.



International Journal of Advanced Research in Electrical, Electronics and Instrumentation Engineering

(An ISO 3297: 2007 Certified Organization)

Vol. 4, Issue 6, June 2015

- [9] Bay, H., Tuytelaars, T., and Van Gool, L., “SURF: speeded up robust features,” in Proc. of Eur. Conf. on Computer Vision (ECCV 2006), pp. 404-417, Springer, Berlin Heidelberg, 2006.
- [10] Dalal, N., Triggs, B., “Histograms of oriented gradients for human detection,” in Proc. of IEEE Conf. on Computer Vision and Pattern Recognition, Vol.1, pp.886–893, 2005.
- [11] Burghouts, G. J., Geusebroek, J. M., “Performance evaluation of local color invariants,” Computer Vision Image Understanding, Vol.113, no.1, pp.48–62, 2009.
- [12] Lu, X. Y., Manduchi, R., “Detection and localization of curbs and stairways using stereo vision,” in Proc. of IEEE Int. Conf. on Robotics and Automation (ICRA 2005), pp.4648–4654, 2005.
- [13] Albert, A., Suppa, M., and Gerth, W., “Detection of stair dimensions for the path planning of a bipedal robot,” in Proc. of IEEE Int. Conf. on Advanced Intelligent Mechatronics, Italy, Como, pp. 1291–1296, 2001.
- [14] Wang, S., Wang, H., “2D staircase detection using real Adaboost,” in Proc. of the 7th Int. Conf. on Information, Communications and Signal Processing (ICICS'09), pp.1–5, 2009.
- [15] Gutmann, J. S., Fukuchi, M., and Fujita, M., “Stair climbing for humanoid robots using stereo vision,” in Proc. of 2004 IEEE/RSJ Int. Conf. on Intelligent Robots and Systems (IROS), Vol. 2, pp.1407–1413, 2004.
- [16] Jarvis, R. A., “A perspective on range-finding techniques for computer vision,” IEEE Trans. Pattern Analysis and Machine Intelligence, vol. 5, pp.122–139, March, 1983.
- [17] Davis, J., Nehab, D., Ramamoorthi, R., and Rusinkiewicz, S., “Spacetime stereo: a unifying framework for depth from triangulation,” IEEE Trans. Pattern Analysis and Machine Intelligence, vol.27, no.2, pp.296–302, Feb. 2005.
- [18] Gachter, S., Nguyen, V., and Siegwart, R., “Results on range image segmentation for service robots,” in Proc. of 4th IEEE Int. Conf. on Computer Vision Systems (ICVS), pp.53, 2006.
- [19] Soquet, N., Aubert, D., and Hautiere N., “Road segmentation supervised by an extended V-disparity algorithm for autonomous navigation,” in Proc. of IEEE Intelligent Vehicle Symposium, pp.160–165, 2007.
- [20] Filipe, V., Fernandes, F., Fernandes, H., Sousa, A., Paredes, H., and Barroso, J., “Blind navigation support system based on Microsoft Kinect,” Procedia Computer Science, Vol. 14, pp.94–101, 2012.
- [21] Delmerico, A. J., Baran, D., David, P., Ryde, J., and Corso, J. J., “Ascending stairway modeling from dense depth imagery for traversability analysis,” Robotics and Automation (ICRA), IEEE Int. Conf. Karlsruhe, Germany, pp.2283–2290, 2013.
- [22] Csaba, G., Somlyai, L., and Vámosy, Z., “Mobile robot navigation in unknown environment using structured light,” in Proc. of 3rd IEEE Int. Symp. on Logistics and Industrial Informatics (LINDI), pp.249–254, 2011.
- [23] Oßwald, S., Gutmann, J.-S., Hornung, A., and Bennewitz, M., “From 3D point clouds to climbing stairs: a comparison of plane segmentation approaches for humanoids,” in Proc. of 11th IEEE-RAS Int. Conf. on Humanoid Robots (Humanoids), pp.93–98, 2011.
- [24] Oßwald, S., Gorog, A., Hornung, A., and Bennewitz, M., “Autonomous climbing of spiral staircases with humanoids,” in Proc. of IEEE/RSJ Int. Conf. on Intelligent Robots and Systems (IROS), pp.4844–4849, 2011.
- [25] Labecki, P., Walas, K., and Kasinski, A., “Autonomous stair climbing with multisensor feedback,” In preprints of the 18th IFAC World Congress, Milano, Italy, IFAC papers online, Vol. 18(1), pp.8159–8164, 2011.